doi:10.1038/nature09934

Supplementary Discussion

Interestingly, a recent study demonstrated that knockdown of Tet1 alone would lead to dys-regulation of differentiation genes, but only minor defects in ES maintenance and no change in expression of pluripotency factor Nanog [1]. We noticed at least three differences between this study and our previous study [2]. First, this study used V6.5 mouse ES cells while we used the E14Tg2A mouse ES cells; Second, this study co-cultured their mouse ES cells with feeders while we cultured ES cells under feeder-free conditions; Third, this study employed transient electroporation of siRNA duplexes to delete Tet1 and achieved only 30% of decrease in 5hmC levels when evaluate at day 5 after transfection, while our study achieved ~65% decrease in 5hmC levels when evaluate FACS-sorted Tet1-depleted E14Tg2A ES cells after 8 days of lentiviral transfection. While it is not clear exactly which of the above differences contributes to the phenotypical differences between this study and our previous results [2], the differences in mouse ES strains (V6.5 vs. E14Tg2A), culturing condition (co-culture with feeders vs. feeder-free conditions) and Tet1 knockdown methods/duration (siRNA electroporation/5 days vs. lentiviral transduction/8 days) can all contribute to the phenotypical differences. It is known that ES cells are more resistant to manipulation when co-cultured with feeders comparing to feeder-free conditions. Consistent with the notion that the differences in the genetic background of V6.5 and E14Tg2A ES cells may also contribute to the phenotypical differences, we found that backcross to the C57BL6 genetic background can relive the embryonic lethal phenotype of Tet1 knockout mice (unpublished observation). Further investigation of mice deficient for Tet1 or Tet2 alone or in combination should reveal the level of redundancy and genetic background-dependent differences in mouse ES cells and early embryonic development.

1. Koh, K.P. et al. Tet1 and tet2 regulate 5-hydroxymethylcytosine production and cell lineage specification in mouse embryonic stem cells. *Cell Stem Cell* **8**, 200-213 (2011).
2. Ito, S. et al. Role of Tet proteins in 5mC to 5hmC conversion, ES-cell self-renewal and inner cell mass specification. *Nature* **466**, 1129-1133 (2010).

Supplementary Figures

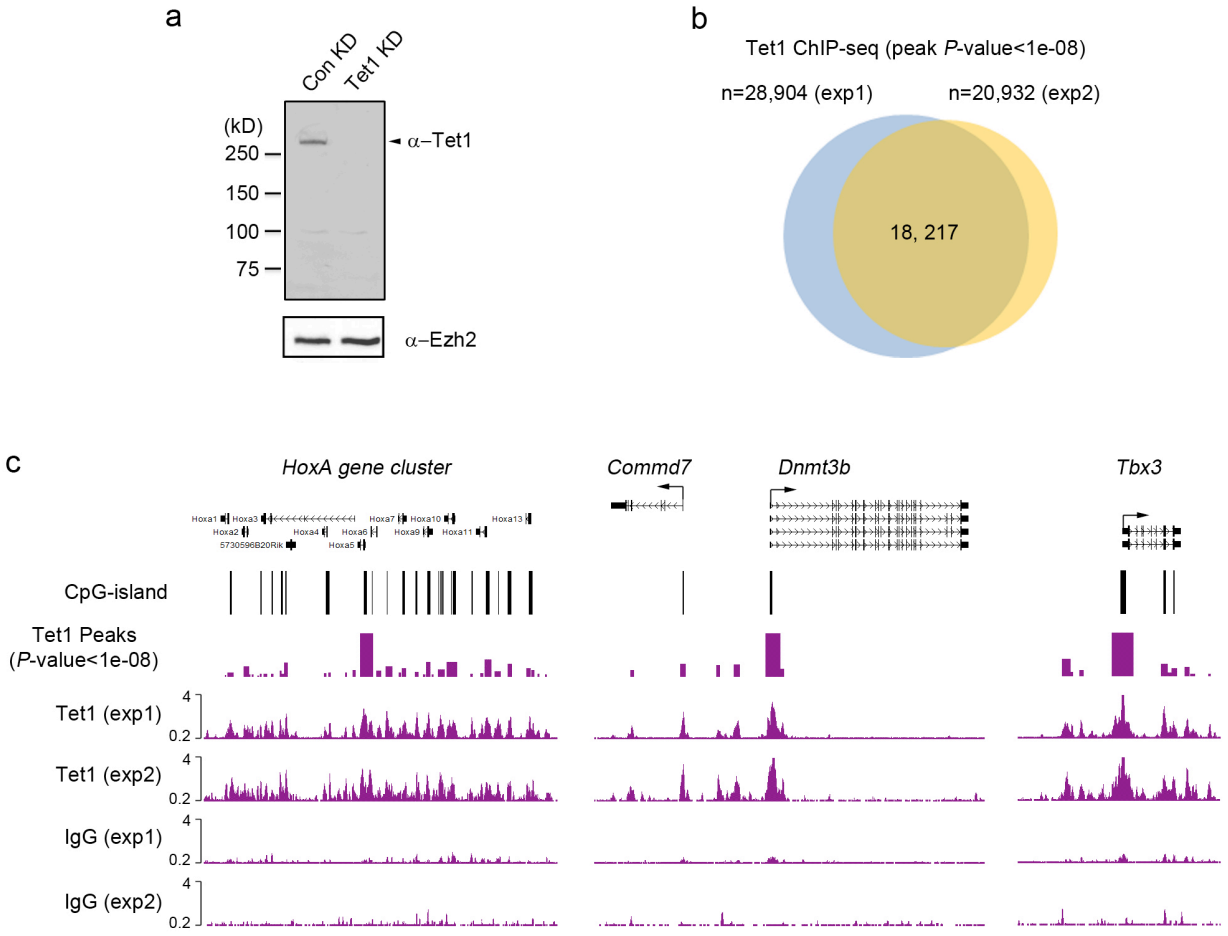

Figure S1. Tet1 ChIP-seq using purified Tet1-specific antibody is highly reproducible

(a) Western blot analysis of Tet1 protein in control (Con KD) and Tet1-depleted (Tet1 KD) mouse ES cells. Ezh2 serves as a control for equal loading as Tet1 knockdown does not affect Ezh2 expression.

(b) A majority of Tet1 peaks (87%) are reproducibly detected in biologically independent samples. Note that exp1 (~35.6 million reads) has four-times reads when compared with that of exp2 (~9.4 million reads). Because the peaks identified from the two experiments are highly reproducible, we identified the Tet1 peaks by combining reads from both experiments.

(c) Representative loci of Tet1 bound regions that were identified by ChIP-seq. Note that the peaks identified in the two independent experiments are highly reproducible.

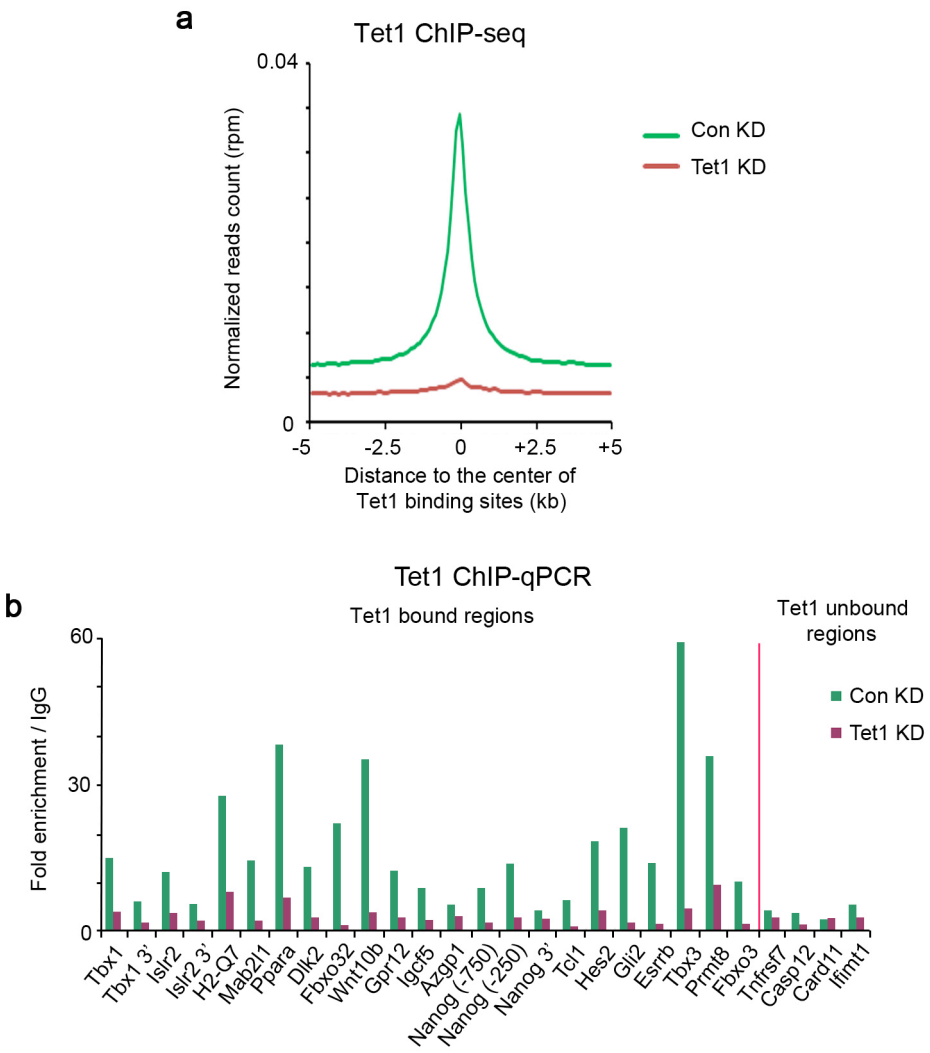

Figure S2. Verification that Tet1 KD affects its binding to chromatin by ChIP assays

(a) Sequencing analysis of genomic DNA immunoprecipitated by Tet1 antibodies in control and Tet1 KD mouse ES cells showed that Tet1 occupancy is generally decreased within Tet1 binding sites in Tet1-depleted cells, confirming the specificity of Tet1 ChIP assays. Rpm, reads per million reads.

(b) ChIP-qPCR analysis confirms the binding of Tet1 to a cohort of randomly selected Tet1 binding-sites identified by ChIP-seq analysis. Shown is the fold of enrichment of Tet1 in control (Con KD) and Tet1-depleted (Tet1 KD) mouse ES cells relative to IgG. The Tet1 unbound regions serve as controls.

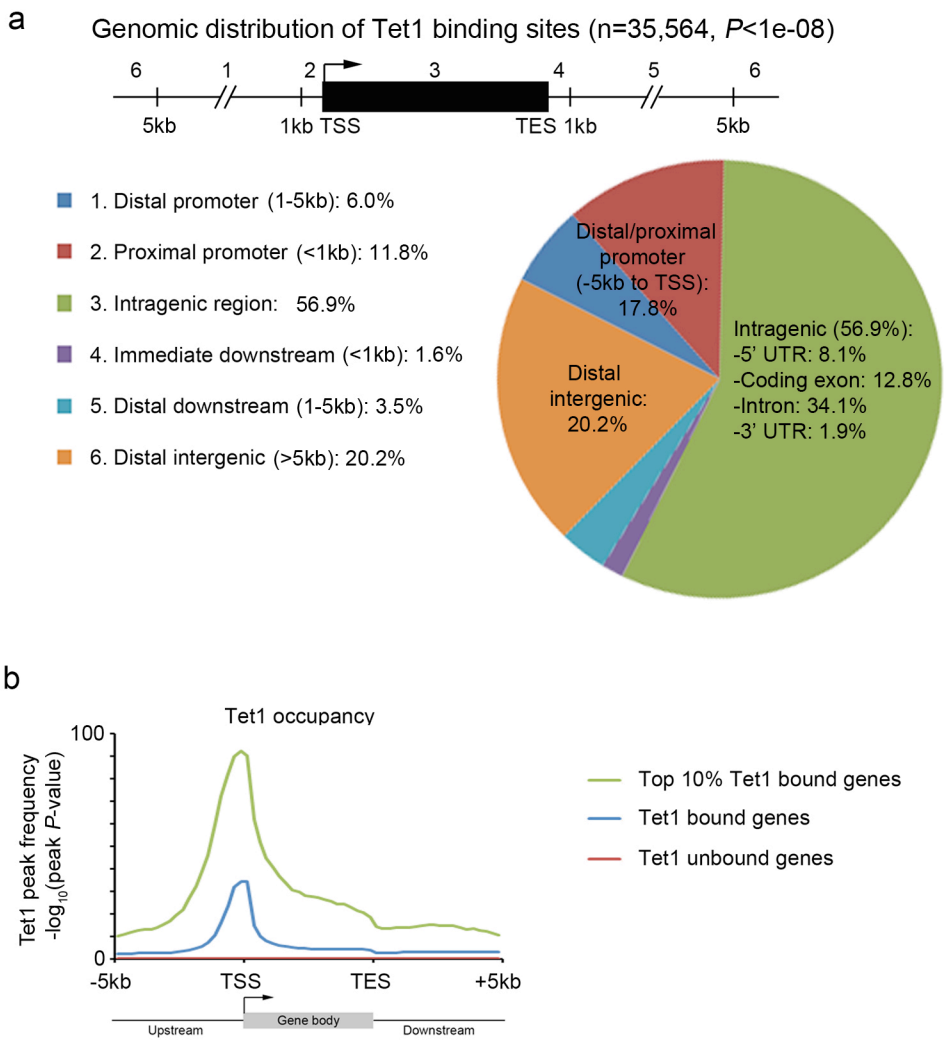

Figure S3. Genomic distribution of Tet1 binding-sites in mouse ES cells

(a) Genomic distribution of Tet1 bound sites (*P*-value < 1e-08 or FDR<1%) relative to UCSC RefSeq genes (NCBI build 36/mm8).The analysis was performed using the cis-regulatory element annotation system (CEAS).

(b) Genome-wide occupancy of Tet1 relative to all annotated genes in ES cells. The genome-wide Tet1 occupancy was determined by ChIP-seq analysis and the significant Tet1 peaks were identified by the MACS program. Averaged Tet1 binding (measured by $-\log_{10}$ (Peak *P*-values) in 200 bp bins up-/down-stream of gene bodies or 5% interval within gene body) is shown along the transcription units from 5-kb upstream of transcriptional start sites (TSS) to 5-kb downstream of the transcriptional end sites (TES). Color coding of the graphs are indicated on the right.

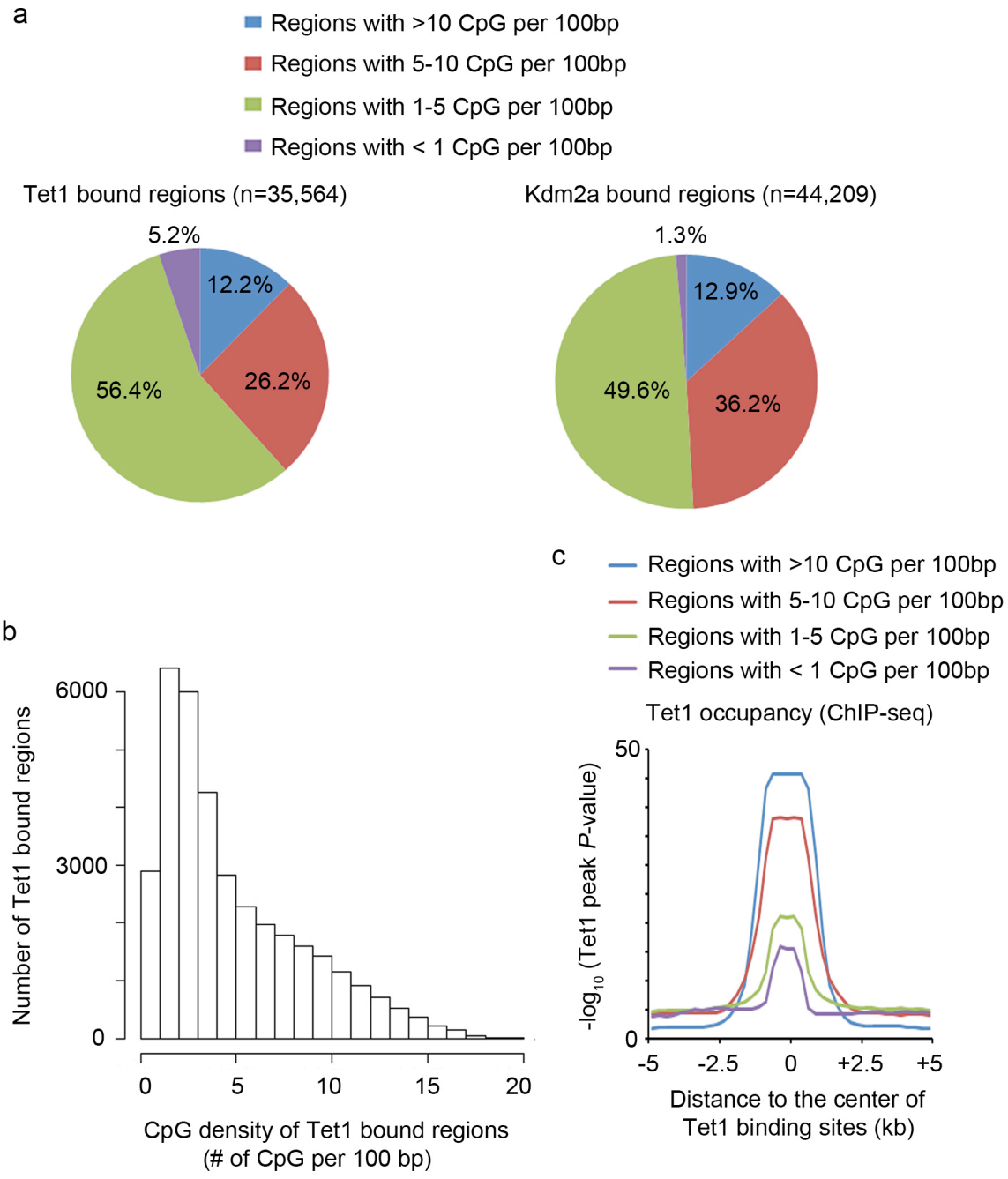

Figure S4. CpG-density distribution of Tet1 binding-sites

(a) Proportion of Tet1 or Kdm2a (Blackedge et al. 2010, Mol Cell) binding-sites with different CpG-density.

(b) Frequency distribution of Tet1 binding-sites with different CpG-density.

(c) Relative enrichment of Tet1 occupancy at binding-sites with different CpG-density.

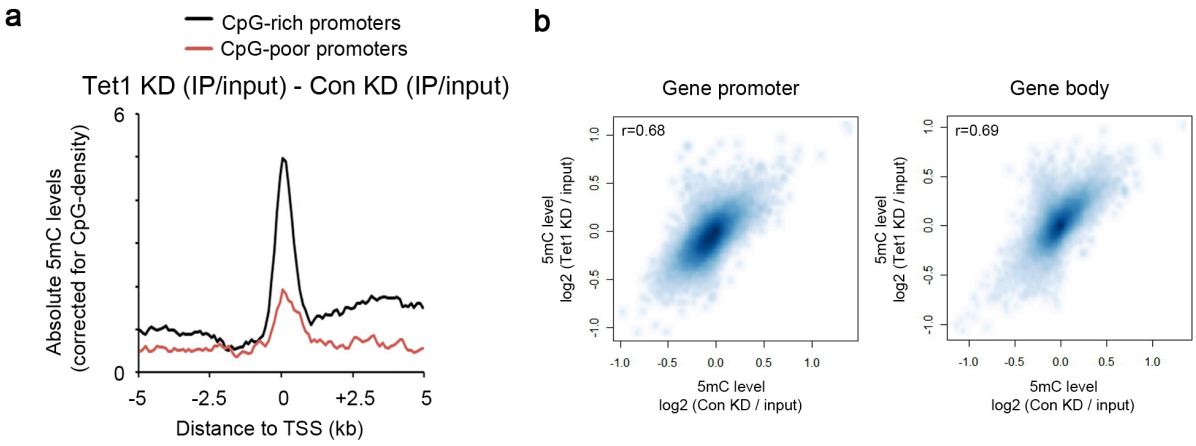

Figure S5. Tet1 is required for maintaining a generally hypomethylated state at a cohort of genomic regions

(a) MeDIP-Chip analysis (IP/input) of 5mC levels in control and Tet1 depleted mouse ES cells are shown for CpG-rich and CpG-poor gene promoters. Note that MeDIP signals were corrected for CpG-density to calculate absolute 5mC levels.

(b) Smooth scatter plot of 5mC levels of Con KD and Tet1 KD cells within gene promoters (-5kb to TSS) or gene bodies. Note that 5mC levels of a fraction of genes are increased in Tet1 KD cells as compared to those of Con KD cells.

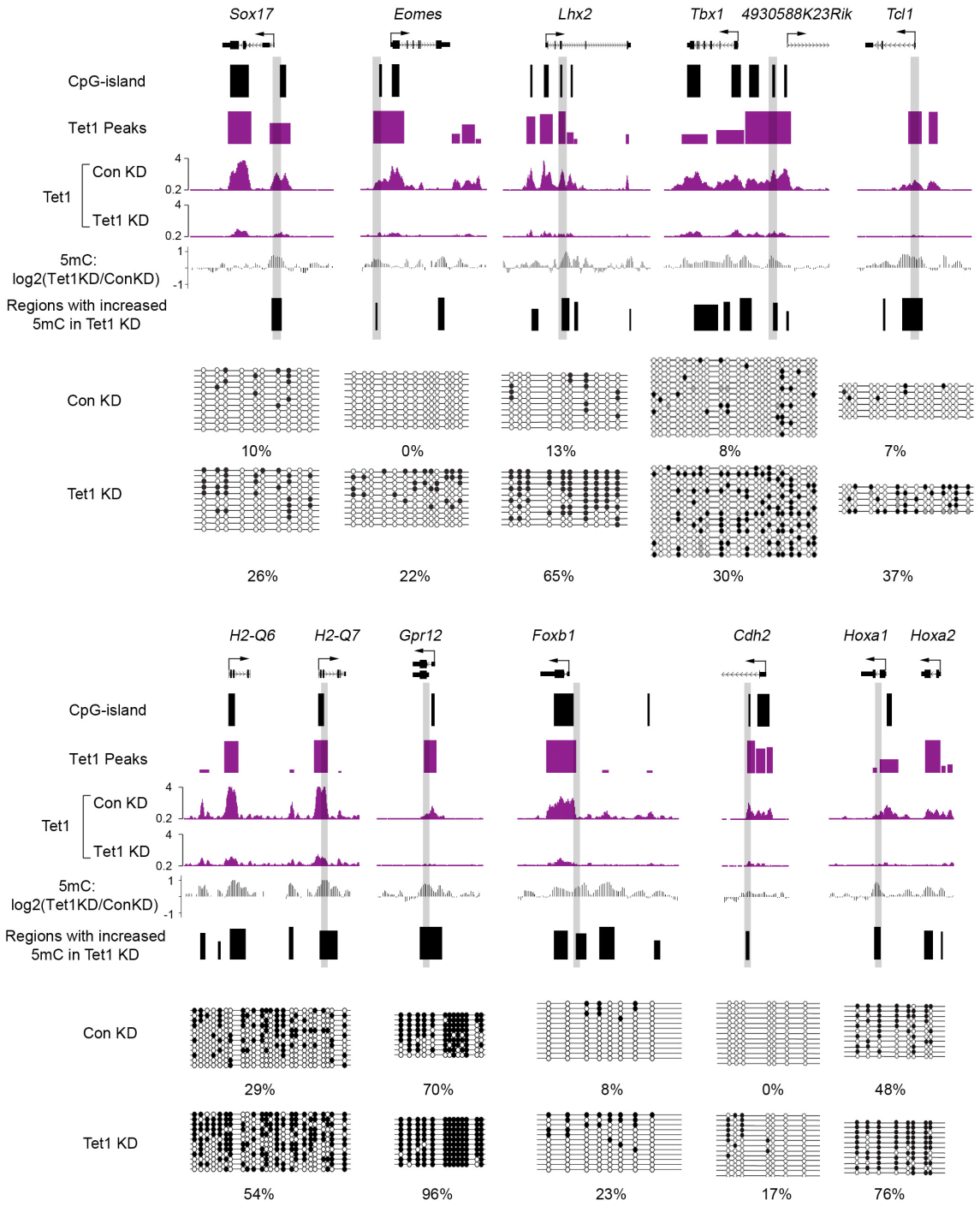

Figure S6. Bisulfite sequencing validation of Tet1-dependent maintenance of a generally hypomethylated state at Tet1 binding-sites

Tet1 occupancy and changes in 5mC levels upon Tet1 KD are shown for representative Tet1 targets. Tet1 ChIP-seq data in Con KD and Tet1 KD are shown in reads per million with the y-axis floor set to 0.2 reads per million. Changes in 5mC levels are shown as log2 ratios of (Tet1 KD / Con KD). Methylation levels of specific genomic regions (shaded in gray) in control and Tet1 KD cells are further analyzed by bisulfite sequencing (lower panels).

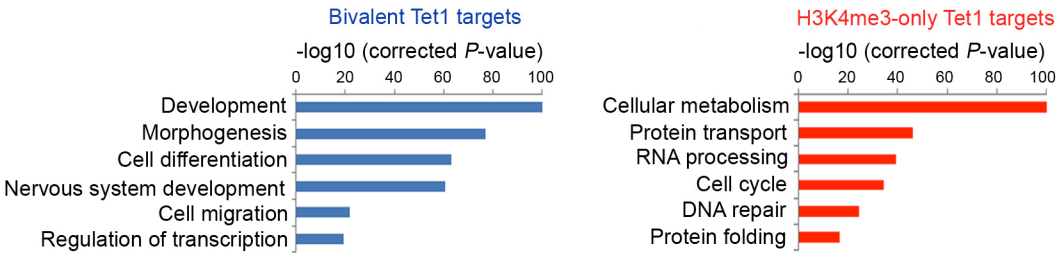

Figure S7. Gene ontology analysis of bivalent and H3K4me3-only Tet1 targets

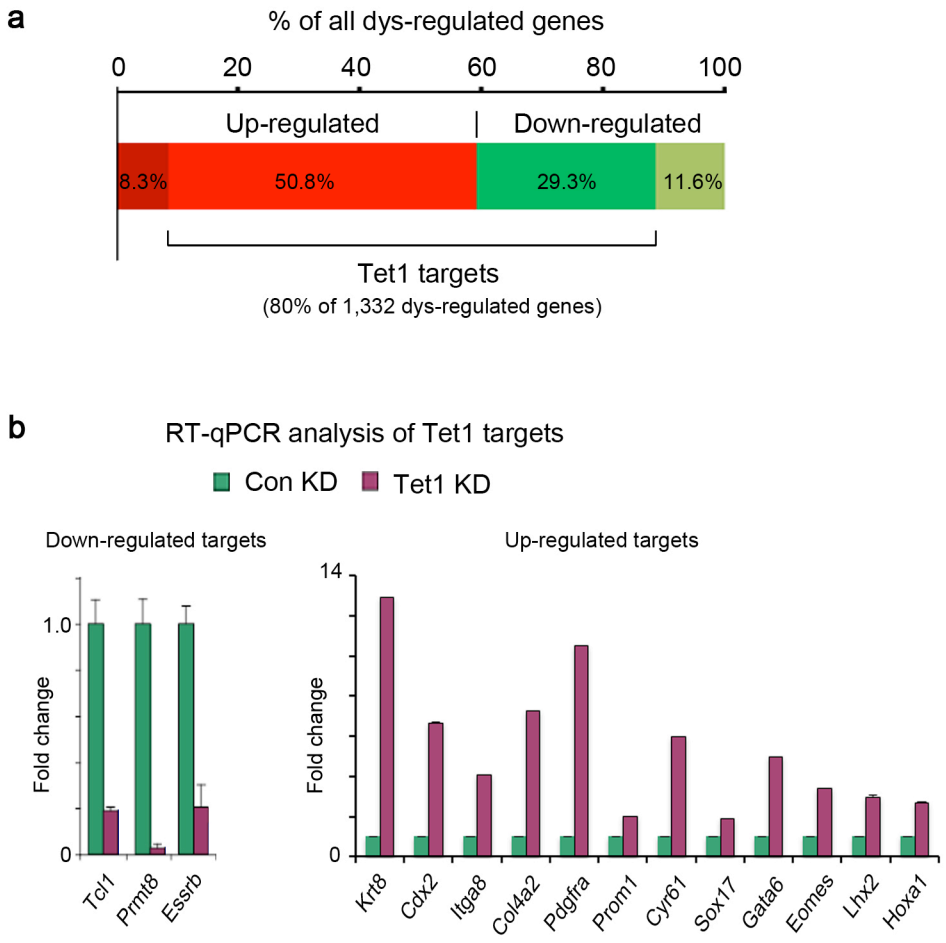

Figure S8. Whole genome transcriptional profiling analysis and verification by qPCR demonstrate Tet1-dependent changes in gene expression

(a) A majority (80%) of dys-regulated genes in Tet1-depleted ES cells are Tet1 direct targets.

(b) RT-qPCR analysis of expression levels of selected H3K4me3-only and bivalent Tet1 targets in control and Tet1 KD ES cells. Error bars represent s.d. determined from duplicate experiments.

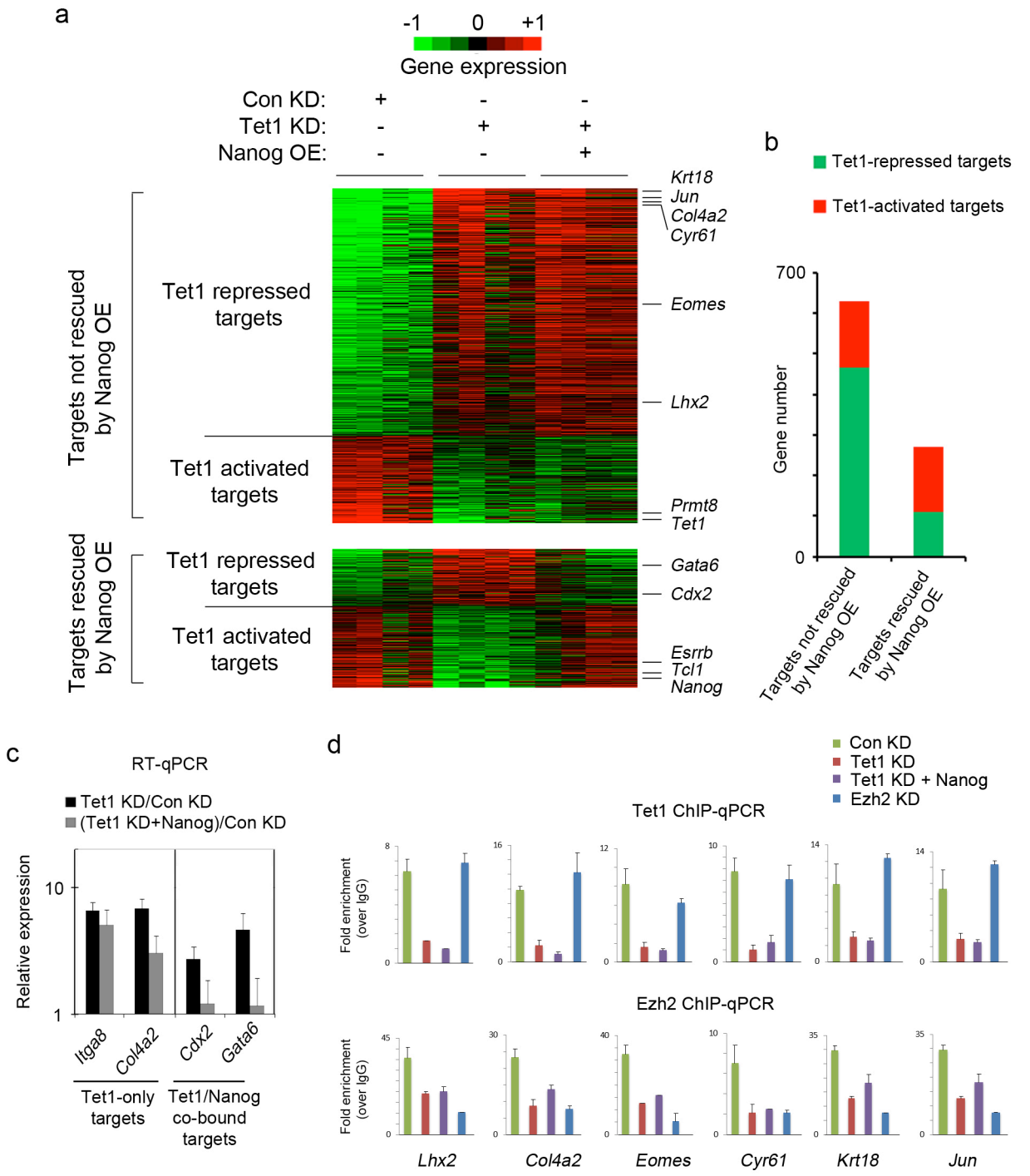

Figure S9. Nanog only rescues a subset of dys-regulated Tet1 targets

(a) Heatmap representation of gene expression profiling in con KD, Tet1 KD and Tet1 KD rescued by Nanog overexpression (OE). Representative genes are indicated on the right.

(b) Summary of gene number for each class of dys-regulated Tet1 targets.

(c) RT-qPCR analysis of selected Tet1 targets in Tet1 KD mouse ES cells and Nanog-rescued Tet1 KD cells. Relative gene expression was normalized to control KD. Note that while two Tet1/Nanog co-bound targets were effectively rescued by overexpression of Nanog in Tet1-

depleted mouse ES cells, upregulation of other Tet1 targets in response to Tet1 KD was not rescued by Nanog overexpression. Error bars represent s.e.m. determined from triplicate experiments.

(d) Shown are ChIP-qPCR analyses of Tet1 and Ezh2 for six Tet1/PRC2 co-bound targets, all of which are dys-regulated in Tet1-depleted cells and not rescued by Nanog overexpression. Note that decreased Ezh2 occupancy on these genes in Tet1 KD cannot be rescued by Nanog overexpression. Error bars represent s.d. determined from duplicate experiments.

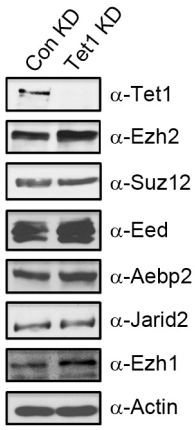

Figure S10. Western blot analysis demonstrates that Tet1 depletion does not affect the protein levels of PRC2 subunits

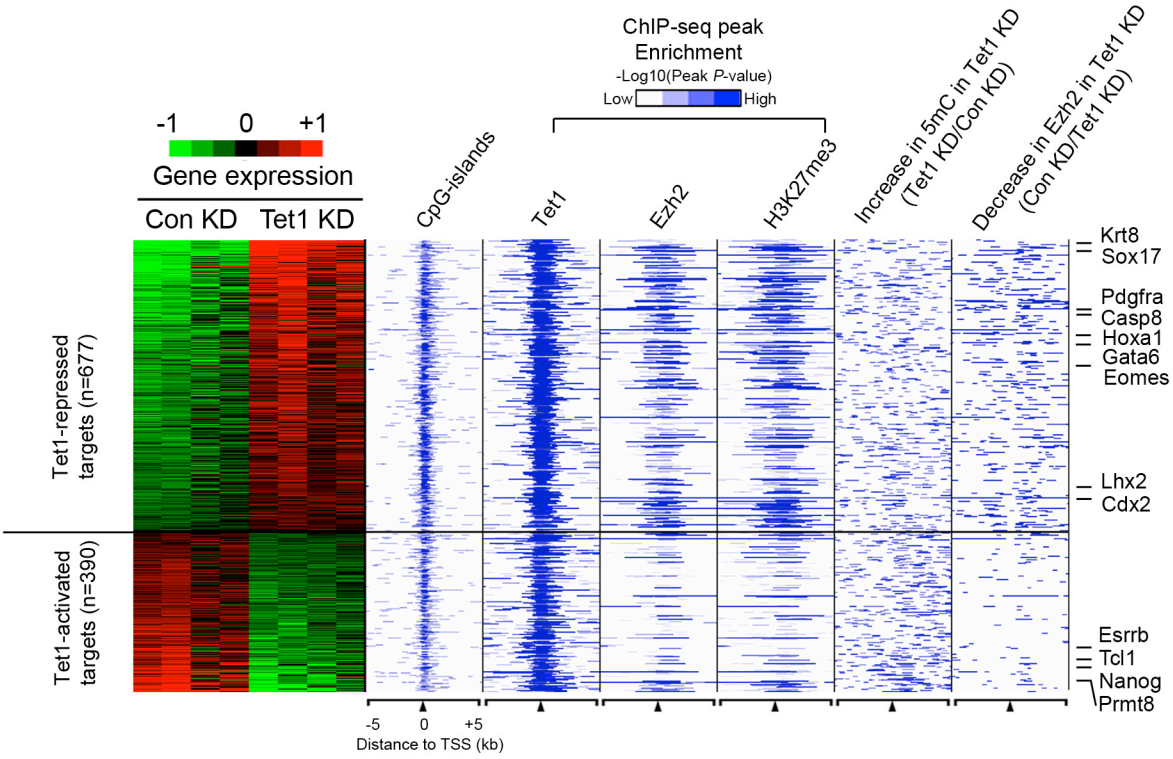

Figure S11. PRC2 occupancy is preferentially reduced in Tet1-repressed targets
Changes in gene expression of Tet1 targets in response to Tet1 knockdown is indicated by heatmap (left). The relationship of these genes to CpG-island, Tet1 binding, Ezh2 binding (Ku et al. 2008, PLoS Genet.), and H3K27me3 (Mikkelsen et al. 2007, Nature) are presented in the middle columns. Changes in 5mC levels and Ezh2 binding in response to Tet1 KD are presented on the right two columns.

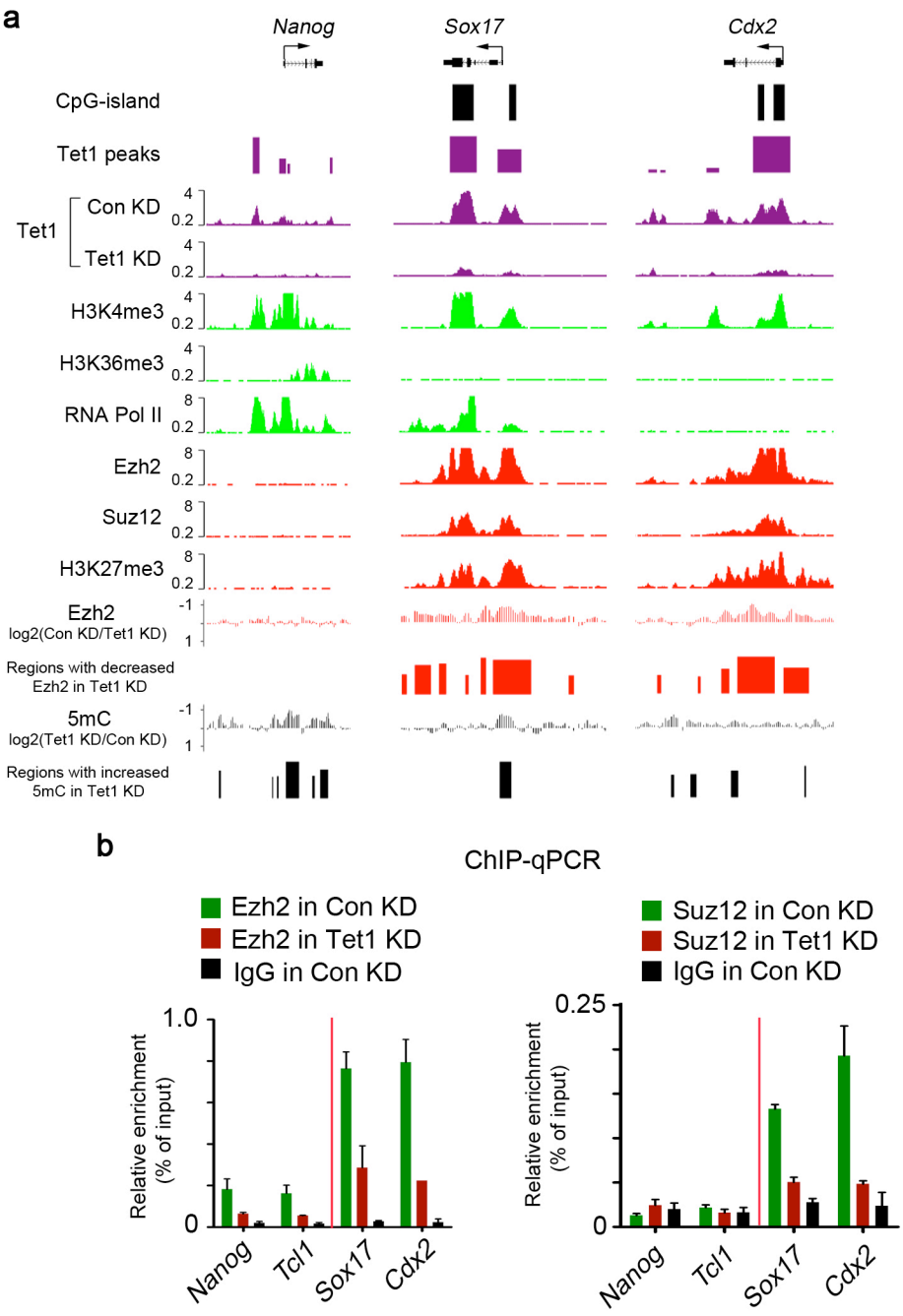

Figure S12. Tet1-depletion in ES cells leads to decrease in PRC2 occupancy at Tet1-repressed bivalent genes

(a) Occupancy of PRC2 (Ku et al. 2008, PLoS Genet.; Mikkelsen et al. 2007, Nature; Seila et al. 2008, Science) on representative Tet1-repressed, but not on Tet1-activated, targets.

(b) ChIP-qPCR analysis demonstrated that Tet1-depletion resulted in decreased Ezh2 and Suz12 occupancy at Tet1-repressed targets (*Sox17* and *Cdx2*), but not at Tet1-activated pluripotency factors (*Nanog* and *Tcl1*). Error bars represent s.e.m. determined from duplicate experiments.

SUPPLEMENTARY TABLE S8. Real-time RT PCR primers

Gene	Strand	Sequence
ITGA8	F	GGCCGTTCTCTGCACGGGAT
	R	CTGGGGAGGCAGCAGGCTTT
PDGFRA	F	AAAGGGAGGACGTTCAAGAC
	R	GTTAAAGACGGCACAGGTCA
CYR61	F	CCAGACTGGCGCTCTCCACC
	R	GCGCAGACCTTACAGCAGCC
GAPDH	F	CATGGCCTTCCGTGTTCCTA
	R	GCCTGCTTCACCACCTTCTT
CDH2	F	CTTCTGCTGCCTCTGCTG
	R	ATTTCACCAGAAGCCTCCAC
GATA6	F	GAGCTGGTGCTACCAAGAGG
	R	TGCAAAAGCCCATCTCTTCT
KRT8	F	AACAACAAGTTCGCCTCCTT
	R	GTTGCTCCTCGACGTCTTCT
COL4A2	F	GCCCCCAGGGTTCATGGGAC
	R	GGCTGGGCCCCTAGCACTTC
PROM1	F	TCCTCAACGTGGTCCAGCCG
	R	AGGGCAATCTCCTTGGAATCAACTG
SOX17	F	GGTCTGAAGTGCGGTTGG
	R	TGTCTTCCCTGTCTTGGTTGA
EOMES	F	CCTCCGTACTTGCTTCTACACACTT
	R	AAAGCCTATAGGAACTGTGACATCATAC
TCL1	F	GGTACCGAAGCTGCGACTCCA
	R	TGCAGGACCGGGTCTGGGTT
PRMT8	F	GCCTGCAGATCCAGCGCAAC
	R	AGGGGGCATCAGGGGCTGTA
ESRRB	F	GCGCAGGTACAAGAAACTCA
	R	CGCCTCCAGGTTCTCAAT
TBX3	F	CAAGGAACTTTGGGACCAGT
	R	TTGGCCTTTTTATCCAGTCC
LHX2	F	TTGCACTTCGAGGCTCTGCTGC
	R	TGGACTCTTGCGCTTTCTCGGC
HOXA1	F	GCGCACCAATTTCACCACCAAGC
	R	GCTTCTTCTGCTTCATGCGGCG

SUPPLEMENTARY TABLE S9. ChIP primers

Gene	Strand	Sequence
NANOG-750	F	GGCCTCTACATTAATTTAAACACTCCTTAA
	R	CAAGTCTGAAGAAAGAGCCTGTGTC
NANOG-215	F	CAGGTTCCTTCCTTCTTCCA
	R	ATGGTGGCTCACAACCATAC
NANOG-3’	F	CAGGTTCCTTCCTTCTTCCA
	R	ATGGTGGCTCACAACCATAC
TBX1	F	ACTCTTAGGACCGCCCTTTC
	R	GAGTGGGTTCGTTCCTTAGC
TBX1-3’	F	GGAGTAGCCCAGCACTCTCT
	R	CTTTCTTGTTGCCTTGGACA
ISLR2	F	CTCTCCCAACTCTGGCTTTC
	R	GTTCCACGGGAATCAGTACC
ISLR2-3’	F	CATGGAGAGGAGGATGGACT
	R	AACGTCACAGGAGAATGCTG
H2-Q7	F	GTGATTACCCGGAACCAATC
	R	AGCAGCATTGTTAGAGCCATT
MAB21L1	F	CAGATGAGCCAAGGAAGACA
	R	CGCCAGATCAACAAGAAAGA
PPARA	F	TTTCTCCCCATTTCTCATCC
	R	TAGATCGCACAGCTTGTTCC
DLK2	F	CTGTGAAAACTGGGAGCAGA
	R	GTCACTGGCTTCGTAGGTCA
FBXO32	F	CCTCTTCTTTCCCCTTCCTT
	R	CCAGGGTGTGCTAAGTGAAA
WNT10B	F	AGAACCACCCGTGAGTTAGG
	R	GAGGAAGGGAGGGTAAAAGG
GPR12	F	GGAGTCGCTTGCTGTTGTAA
	R	CTCGGCTTCTTATGCTTTCC
IGCF5	F	CAGGTGCTGAGAATGTTGGT
	R	CGGTCTGCTCTCCTAGCTCT
AZGP1	F	GGAGCCACTGGTCTATGGAT
	R	GAAAGGGTGGGGTCTAGTGA
TCL1	F	TGCAATTTTCTGCTTCTTGC
	R	GTACACGTGCTTCTCCCAGA
HES2	F	GCTCCTCAAGCACCTCCTAC
	R	TGTTGCAATTTTGGGACAGT
GLI2	F	GTGTGCTCCTGTAGCTGGAA
	R	GCCACTCTGGAGGAGAAGAG
ESRRB	F	CCAGCTCGATTCTGTCACTT
	R	TTGGAGCCCACTAACCCTAC
TBX3	F	GCTTATTGGCCGAAAGAGAG
	R	CCGAGCGCTACAGTTCAAG

PRMT8	F	GTTCATGCCCCAAACAGTAA
	R	GTCCTTCTAACGAGGGCAAG
FBXO3	F	CAAAGGCCAGGTAGGGTTAG
	R	GTCCCTGCCAGTCTGTTTCT
TNFRSF7	F	CAGTTGTGGCTGTTTTGGTT
	R	GGCACATGTCTGTGAAGCTC
CASP12	F	TGACGTACCTGGGTTTTGAA
	R	ATGAGACCATGAGACCGTGA
CARD11	F	CCACATCCCACTTCTTCCTT
	R	AGCTTGTGGGAAGCAGAGAT
IFITM1	F	TGACAAGTTGTGTGCTCCTG
	R	TCCCCAGTGCATAGGTTACA
SOX17	F	TTTTCTCTGTCTTCCCTGTCTTGG
	R	CGGGCTTTCTTTCTAACCACTTTC
LHX2	F	CCACAGGCTTGGATCTGTTA
	R	CTAGGAGGGGAAGGGAAATC
CYR61	F	CATCGTTCAGACCACGTCTT
	R	CAAGGACGCACTTCACAGAT
HOXA1	F	AACCGAATATTGCCTCAAGC
	R	CACGTAGCCGTACTCTCCAA
EOMES	F	CACCCTTTGAGGGGAATAAA
	R	AGAGAACTCGGGCTGACATC
PCDH8	F	TGGACACGCACGTCAAGCTG
	R	TGGGTCGCAACGGTCAAGTCAC
GATA6	F	ATCATGTCTGGAGCGGTTTT
	R	TCTCCTTCTCTCTCCCTTCG
CDX2	F	CAGTTTGGCCATTAGGGTCT
	R	CACTTCCTCCGAGGCTTCT
JUN	F	GACTGCAAAGATGGAAACGA
	R	CAAGGTCATGCTCTGTTTTAGG
KRT18	F	GTGCACTGCCTCCTAGAAGAT
	R	TGGTTGGGTGACTTCAGAAA
COL4A2	F	CAGCACCAGAGGAAACAAAA
	R	GAGTGCGTGCCTGAAAATTA

SUPPLEMENTARY TABLE S10. Bisulfite Sequencing primers

Gene	Strand	Sequence
NANOG	F1	GAGGATGTTTTTTAAGTTTTTTTT
	F2	AATGTTTATGGTGGATTTTGTAGGT
	R	CCCACACTCATATCAATATAATAAC
TCL1	F1	TTGGGGGTTTTGAAGAATTTT
	R1	ACACAAAAAACCCTCTATATC
	F2	AGTTTAGATTTTGTTTTTGTTTTA
	R2	AAACCCAAACAAAACATATCC
TBX1	F1	GAAGAGGATATAATTTAGGTTT
	R1	TTACTATAAAAAATTAAAACCCC
	F2	GGTGTAAGTTTAGGATTTTTG
	R2	CCCCTAAAAAAACTAACTTAAA
H2-Q7	F	AGGAGGGATTGATTATTGGGTTT
	R	ACTAAAAATTTCTTCTTCCCCAAAA
GPR12	F	GTTAGGAAGTGGTGTTGTAGGGTTA
	R	TTCAATCAAAAACCACCAAACTAAT
FOXB1	F	TTTTTAGGTTAAGGTAAGTTTGGGG
	R	TCTCAACAAACACTATTTATCTTTTCA
CHD2	F1	TATATTTTTATTAGGAGGAGAG
	R1	AAAAAAAAAAAACCAAAAAACCC
	F2	TTAGTAGGGTGGTAGTTTTAA
	R2	AAAAAAAAAAAACCAAAAAACCC
CYR61	F1	GTAGAAATGTTTTTTTGGTTTG
	R1	TTAACCACTATACATAATATTAAA
	F2	TTTTTATTTTTTTAGTTTTTGGTAT
	R2	CCCACCTATAAAATCATCAC
EOMES	F1	GGATTTTATTTTTGGTTGTGTT
	R1	CTTCATAAACTTAAATACTATATA
	F2	TTTTAGTTATTTTATTTGTAGATAA
	R2	AATATTTTAAAACAACAACCTTAT
HOXA1	F1	TTTGTTAATATTTATAAGGTTTTAT
	R1	TTCTAAAACCAAATCTTCACC
	F2	ATTTTAGGTTAATATTGTTTATATA
	R2	TAAATCTCATTAAACTATAAAAAC
SOX17	F1	ATTTTGTGTAATTGGATTTGAAT
	R1	CTAAAAATTTACTAAAATAAAAATAA
	F2	GGTTTTGGTTATTAGAATATTAA
	R2	ATATCTAAACTAAAAACCTAACA
LHX2	F1	GGGAGATTAATAGTTTTAGGT
	R1	TATAATTTACCCTAAAAAAAAAAAA
	F2	TTTTAGGGTTATAGGTTTGGA
	R2	AATTTATTATTACAAACTTAAAAAAA